Int. J. Heat Mass Transfer. Vol. 26, No. 1, pp. 133–143, 1983
Printed in Great Britain

0017-9310/83/010133-11 $03.00/0

NATURAL CONVECTION EXPERIMENTS IN AN ENCLOSURE BETWEEN ECCENTRIC OR CONCENTRIC VERTICAL CYLINDERS OF DIFFERENT HEIGHT AND DIAMETER

E. M. SPARROW and M. CHARMCHI
Department of Mechanical Engineering, University of Minnesota, Minneapolis, MN 55455, U.S.A.

(*Received* 16 *March* 1982 *and in revised form* 23 *June* 1982)

Abstract—Heat transfer coefficients were determined experimentally for natural convection in the enclosed space between two vertical cylinders maintained at different uniform temperatures. The cylinders were of different height as well as of different diameter. During the course of the experiments, the vertical positioning (i.e. elevation) of the inner cylinder and its eccentricity were varied parametrically. For each enclosure configuration, the inner cylinder Rayleigh number ranged between 1.5×10^3 and 10^5. The heat transfer medium was air. To supplement the experimental work, numerical results obtained from finite difference solutions are presented for the concentric case. Comparisons between the experimental and numerical results yielded agreement which, for the most part, was within 1%. In general, the average Nusselt number was nearly independent of both the elevation and eccentricity of the inner cylinder. This finding enabled the Nusselt number to be correlated as a function of the Rayleigh number and the cylinder-to-cylinder diameter ratio, without regard to elevation and eccentricity.

NOMENCLATURE

A_i, surface area of inner cylinder;
A_o, surface area of outer cylinder;
D_i, inner cylinder diameter;
D_o, outer cylinder diameter;
g, acceleration of gravity;
$\bar{h}_i$, average inner cylinder heat transfer coefficient;
$\bar{h}_o$, average outer cylinder heat transfer coefficient;
H_i, inner cylinder height;
H_o, outer cylinder height;
k, thermal conductivity;
Nu_i, local inner cylinder Nusselt number;
$\overline{Nu}_i$, average inner cylinder Nusselt number;
$\overline{Nu}_o$, average outer cylinder Nusselt number;
Pr, Prandtl number;
Q_{conv}, convective heat transfer rate;
Q_{elect}, electric power input;
Q_{loss}, heat loss through leads;
Q_{rad}, radiation heat transfer between cylinders;
Ra_i, inner cylinder Rayleigh number;
r, radial coordinate;
r_c, radial coordinate of center of inner cylinder;
T, fluid temperature;
T_i, inner cylinder temperature;
T_o, outer cylinder temperature;
z_c, axial coordinate of center of inner cylinder;
z', axial coordinate measured from bottom of inner cylinder.

Greek symbols

β, coefficient of thermal expansion;
ε_i, inner cylinder emissivity;
θ, dimensionless temperature, $(T-T_o)/(T_i-T_o)$;
ν, kinematic viscosity;
σ, Stefan–Boltzmann constant;
Ψ, dimensionless stream function, $\psi/\nu D_o$;
ψ, stream function.

INTRODUCTION

NATURAL convection in enclosed spaces has been studied extensively in recent years in response to energy-related applications (e.g. nuclear, solar, conservation). The enclosures encountered in these and other applications are highly diverse in their geometrical configuration, and only a select few have been investigated in detail. The most investigated enclosures include the annulus between horizontal cylinders, the spherical annulus, the closed rectangular cavity, and the hollow horizontal cylinder. Literature relevant to these cases has been cited [1, 2]. Other enclosures have been investigated to a lesser extent [1, 2], and a number of interesting enclosure configurations have yet to be studied, including that which is the subject of this paper.

Attention is focused here on natural convection in the space between two vertical cylinders of finite height. The respective cylinders are of different height, so that the flow space includes the regions above and below the inner cylinder as well as the annular region between the cylindrical walls. The investigated enclosure configurations encompass both concentric and eccentric positioning of the inner cylinder with respect to the outer cylinder.

A schematic diagram of the physical situation is presented in Fig. 1 in both top and side views. As seen there, the walls of the inner cylinder are maintained at a uniform temperature T_i, while for the outer cylinder the walls are at a different uniform temperature T_o. The height and diameter of the respective cylinders are H_i, D_i and H_o, D_o, and the position of the inner cylinder

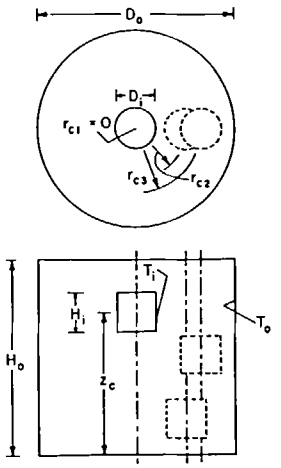

FIG. 1. Schematic diagram of an enclosure bounded by concentric or eccentric vertical cylinders of different height and diameter.

is specified by the axial and radial coordinates z_c and r_c of its center point. In the figure, the inner cylinder is pictured in several representative positions. In all of the work reported here, each of the cylinders is of unit aspect ratio, that is, $H_i = D_i$ and $H_o = D_o$.

In its entirety, the investigation of the enclosure described in Fig. 1 and in the preceding paragraphs included both experiment and analysis. The experimental work, which is the main focus of this paper, encompassed variations of the elevation of the inner cylinder both for the concentric and eccentric modes. In the eccentric case, the fluid flow and temperature field in the enclosure are 3-dim. At each inner cylinder position specified by z_c and r_c, the Rayleigh number was varied over a range of nearly two orders of magnitude. All of the experiments were performed with air as the heat transfer medium and with a fixed ratio of the cylinder diameters $D_i/D_o = 0.2$.

The analytical work consisted of axisymmetric finite difference solutions, with the inner cylinder positioned concentrically. These solutions yielded heat transfer results for comparison with the concentric-mode results of the experiments. The solutions also provided information about the velocity and temperature fields and about the distribution of the local heat transfer coefficient which was not available from the experiments. In addition, the numerical work encompassed cylinder diameter ratios D_i/D_o of 0.1 and 0.3, besides the value $D_i/D_o = 0.2$ which was in common with the experiments.

From the foregoing, it is evident that the experimental and analytical phases of the work provide both comparative and nonoverlapping information. The research, especially the numerical part, has produced a superabundance of results that cannot be conveyed in a paper which conforms to journal length limitations. Therefore, the major part of the analytical work has been reported elsewhere [2]. The present paper is primarily experimental but includes a presentation of analytical results which correspond to the operating conditions of the experiments (i.e. $D_i/D_o = 0.2$). These analytical results were not presented in ref. [2] so that they would be available to be included here along with the experimental data.

In the experiments, the inner cylinder was electrically heated while the outer cylinder was water cooled, so that $T_i > T_o$. From the measurements, average heat transfer coefficients and Nusselt numbers were determined for both the inner and outer cylinders. These results were obtained for inner cylinder elevations z_c/H_o between 0.1375 and 0.8625 at each of the three radial stations $r_c/D_o = 0$, 0.25, and 0.325 depicted in Fig. 1 (note that $H_o = D_o$). The inner cylinder Rayleigh number Ra_i ranged from 1.5×10^3 to 10^5. The analytical results to be presented here include local and average Nusselt numbers, and streamline and isotherm maps for the flow space.

THE EXPERIMENTS

Experimental apparatus

A schematic diagram of the experimental setup is presented in Fig. 2. The components shown in the figure include the inner and outer cylinders which define the enclosure for the natural convection flow, a platform which supports the outer cylinder from below, and a conduit which serves to convey the inner cylinder thermocouple and power leads and to house the inner cylinder suspension line. These components are situated in a large water bath which maintains the temperature of the outer cylinder at a uniform, time-independent value and which also serves as a heat sink for the power supplied to the system. The instrumentation and electric power supply are not shown in the figure but will be described later.

The basic principle underlying the design of the apparatus was the avoidance of spurious heat flow paths from the inner cylinder to the outer cylinder or to the surroundings. Thus, in contrast to other studies of two-body natural convection enclosures, a rigid metallic or non-metallic support was not employed

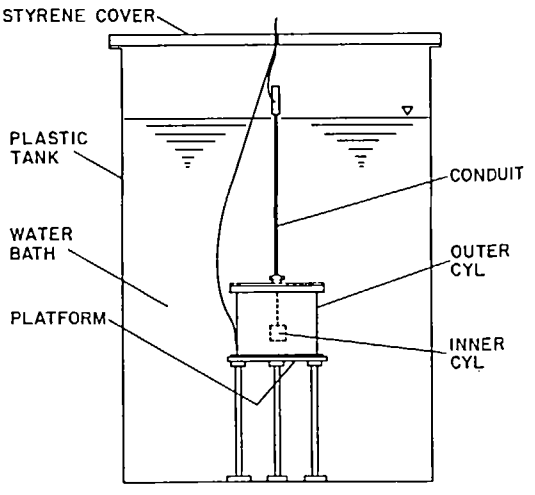

FIG. 2. The experimental setup.

here to position the inner cylinder. Rather, the cylinder was suspended from a 0.046 cm diameter catgut line of the type used in bows. Catgut was chosen because of its ability to totally resist elongation when loaded with the weight of the inner cylinder.

In addition to the inner cylinder support arrangement, other potential thermal bridges between the inner and outer cylinders are the lead wires for the inner cylinder thermocouples and electrical heating element. The thermal conductivities of all common thermocouple pairs were examined, and chromel–constantan was found to have the lowest value. By happy coincidence, chromel–constantan also possesses the greatest thermoelectric sensitivity (emf/degree) and, furthermore, neither chromel nor constantan is attacked by water. The selected chromel–constantan thermocouples were of the smallest diameter that could be handled conveniently, 0.00762 cm diameter with a 0.00762 cm thick Teflon covering.

Of greater concern is the possible thermal bridge provided by the copper lead wires for the heating element. The obvious approach to minimizing conduction along the copper leads is to use wire of very small diameter but, when too small a diameter is used, ohmic heating can become a factor. Thus, a compromise must be sought between the heat conduction and the ohmic heating. This issue was addressed with the aid of the analytical model described in Appendix C of ref. [1]. On this basis, the selected copper lead wire was 0.00762 cm in diameter, with 0.00762 cm thick Teflon insulation.

Various aspects of the experimental apparatus will now be described, but numerous fine details will be omitted to conserve space (see ref. [1] for a more detailed description). The outer cylinder was made entirely of 0.635 cm thick copper, with the internal diameter and height both equal to 15.595 cm. All internal surfaces were carefully machined and finished to ensure trueness and smoothness. The cylinder was assembled from three parts. The cylindrical side wall was permanently mated to the base plate by silver solder. However, the top plate was made removable to allow access to the enclosure. To facilitate the top closure, a ring-like flange was silver soldered to the cylindrical wall at its upper end. An O-ring, compressed when screws were tightened to press the top plate against the flange, ensured a positive seal between the top plate and the cylindrical side wall.

The inner cylinder was also assembled from three parts, all of aluminum. The main body was a cylinder into which a cavity had been machined concentric with the axis, leaving a metal thickness of 0.635 cm for the cylindrical side wall and the closed end wall. The cavity served to house a heater, which consisted of a cylindrical shell into which had been milled an array of 40 equally spaced longitudinal grooves (20 grooves on the outer surface of the shell and 20 grooves on the inner surface). Heating wire, 0.0076 cm diameter chromel coated with 0.0076 cm thick Teflon, was wound in series in the grooves and fixed in place with copper oxide cement. The upward-facing open end of the cavity was closed by a 0.635 cm thick disk having a diameter equal to that of the main body of the cylinder. When assembled, the height and diameter of the cylinder were both equal to 3.119 cm, which is exactly one-fifth the height and diameter of the outer cylinder.

The exposed surfaces of the inner cylinder were subjected to a succession of lapping and polishing operations using 600, 900, and 1200 grit lapping compounds. These operations produced a surface finish which can be characterized as 'highly polished' from the standpoint of thermal radiation properties.

The disk which formed the upper portion of the inner cylinder was fabricated with a concentric cylindrical boss which protruded downward into the hollow core of the heater. A 0.1 cm diameter circular hole was drilled through the disk and the boss, coincident with their axis. The catgut suspension line was drawn through this hole, and the free end of the line which emerged from the boss was threaded through a small hollow spherical ball (from a key chain) and knotted below the ball. When the cylinder was suspended, the ball centered itself in the mouth of the hole. The thermocouple and heater wires were also drawn through the hole, but they were led out via a lateral aperture in the boss in order to circumvent the blockage of the bottom of the hole by the spherical ball.

The lead wires and suspension line passed vertically upward through the intercylinder space as shown schematically in Fig. 2 and entered the conduit via an aperture in the upper wall of the outer cylinder. The conduit was a 38 cm long brass tube, the upper 7.6 cm of which protruded above the surface of the water. A specially designed clamp situated at the upper end of the conduit served to positively position the suspension line. The lead wires emerged from the conduit at a point above the water level and passed to the instrument panel (not shown) via an aperture in the polystyrene sheet which served to insulate the upper surface of the water bath.

As shown in Fig. 2, the conduit is coincident with the axis of the enclosure. To accommodate the eccentric-mode experiments illustrated in Fig. 1, the conduit was successively repositioned to off-axis stations corresponding to $r_c/D_o = 0.25$ and 0.325. For each repositioning, a new aperture was opened in the upper wall of the outer cylinder, and the aperture associated with the former position was closed with a copper plug.

The platform used to support the outer cylinder was a lap-equipped brass ring designed to allow maximum contact between the lower face of the cylinder and the water. The platform was, in turn, supported by three legs. Each leg was independently adjustable, enabling the apparatus to be precisely leveled.

The water bath was contained in a 208 l (55 gal) capacity polyethylene drum. For the fill height used in the experiments, the water provided a heat capacity of 750 kJ $°C^{-1}$ (395 Btu $°F^{-1}$). Thus, for the input powers employed in the experiments (0.09–1.76 W) and with about 2.5 h required to achieve steady state, the

temperature rise of the water during any data run was negligible. In general, since the experiments were performed in a temperature-controlled room, the water temperature was virtually unchanged during the entire course of the research.

Instrumentation and power supply

All thermocouples used in the experiments were made from Teflon-covered 0.0076 cm diameter chromel–constantan wire. The thermocouples were calibrated prior to their installation in the apparatus. In all cases, the thermocouples were installed in the cylinder walls so that the junction was within 0.076 cm of the bounding surface of the enclosure. Copper oxide cement was used to fix the thermocouples in place.

Two thermocouples were installed in the inner cylinder, one each in the upper and lower walls. For all data runs, these thermocouples consistently read identical values within the 1 μV resolving power of the instrumentation. A total of eleven thermocouples were positioned in the top, side, and lower walls of the outer cylinder. For all operating conditions except at the highest power settings, temperature uniformity prevailed on all walls. At the highest power setting (a cylinder-to-cylinder temperature difference of 44.5°C), a bottom-to-top temperature increase of 0.11°C was noted if the water bath was not stirred. When the bath was stirred, temperature uniformity was restored.

The heater power was supplied by a programmable DC source. Within the resolving power of the instrumentation, the voltage provided by the power supply was constant throughout the entirety of each data run. The heater voltage was read directly, while the heater current was measured in terms of the voltage drop across a calibrated shunt.

DATA REDUCTION

The experimental data enabled evaluation of the average heat transfer coefficient and Nusselt number at either the inner cylinder or the outer cylinder. For the inner cylinder (subscript i)

$$\bar{h}_i = Q_{conv}/A_i(T_i - T_o), \quad \overline{Nu}_i = \bar{h}_i D_i/k \tag{1}$$

and for the outer cylinder (subscript o)

$$\bar{h}_o = Q_{conv}/A_o(T_i - T_o), \quad \overline{Nu}_o = \bar{h}_o D_o/k. \tag{2}$$

Since $A_i = 3\pi D_i^2/2$ and $A_o = 3\pi D_o^2/2$ in the present experiments, it follows that

$$\overline{Nu}_o = (D_i/D_o)\overline{Nu}_i. \tag{3}$$

In light of equation (3), there is no need to give separate consideration to $\overline{Nu}_i$ and $\overline{Nu}_o$, and attention will subsequently be focused on $\overline{Nu}_i$.

For the evaluation of $\bar{h}_i$ and $\overline{Nu}_i$ from equation (1), the temperatures T_i and T_o were measured directly as discussed earlier. For Q_{conv},

$$Q_{conv} = Q_{elect} - Q_{rad} - Q_{loss} \tag{4}$$

in which the electrical input Q_{elect} was obtained from the measured heater voltage and current, while Q_{rad} and Q_{loss} are calculated corrections. With regard to radiation, it is relevant to note that the surface area ratio $A_i/A_o = 0.04$ and that, furthermore, the surface of the outer cylinder which bounds the enclosure is isothermal. Therefore, the radiation problem can be accurately modeled as that of a small body in a large isothermal-walled enclosure [3], so that

$$Q_{rad} = \varepsilon_i A_i \sigma(T_i^4 - T_o^4). \tag{5}$$

In accordance with the highly polished aluminum surface of the inner cylinder, ε_i was taken as 0.05. In general, Q_{rad} was about 5% of the electric power input.

The quantity Q_{loss} takes account of heat transfer through the lead wires which bridge between the inner and outer cylinders. (In actuality, only the copper leads need be considered.) The analysis to determine Q_{loss}, which is detailed in Appendix C of ref. [1], took account of conduction and ohmic heating in the leads and of convection at the surface of the leads. It was found that Q_{loss} was entirely negligible except at the highest elevations of the inner cylinder, and even then it was small. For example, for $z_c/H_o = 0.8625$, Q_{loss} ranged from 4 to 2% of the power input over the range from $Ra_i = 1.5 \times 10^3$ to 10^5.

The $\overline{Nu}_i$ results will be presented as a function of the inner cylinder Rayleigh number

$$Ra_i = [g\beta(T_i - T_o)D_i^3/\nu^2]Pr. \tag{6}$$

The thermophysical properties which appear in equation (6), as well as the thermal conductivity in the Nusselt number, were evaluated at the mean temperature $\frac{1}{2}(T_i + T_o)$.

EXPERIMENTAL RESULTS

The first part of the presentation of the experimental results will focus on those cases for which corresponding analytical results are available for comparison. The predictions of the numerical solutions for $\overline{Nu}_i$ are listed in Table 3 of ref. [2]. As noted earlier, the numerical work was carried out for the concentric case ($r_c/D_o = 0$). Three inner cylinder elevations were considered, $z_c/H_o = 0.25, 0.5$, and 0.75. These, then, are the cases for which comparisons will be made between experiment and analysis.

The comparisons are shown in Fig. 3, where $\overline{Nu}_i$ is plotted as a function of Ra_i. The figure is subdivided into three graphs, each for a different value of z_c/H_o. Inspection of the figure reveals excellent agreement between the numerical predictions and the experimental data. Among the 22 data points, the great majority fall within 1% of the prediction lines, and the largest deviation is 3% (two data points).

The remarkable agreement in evidence in Fig. 3 lends support both to the experimental technique and to the methodology used in the numerical solutions. This validation of the numerical work extends, by inference, to the entire range of Ra_i and D_i/D_o investigated in refs.

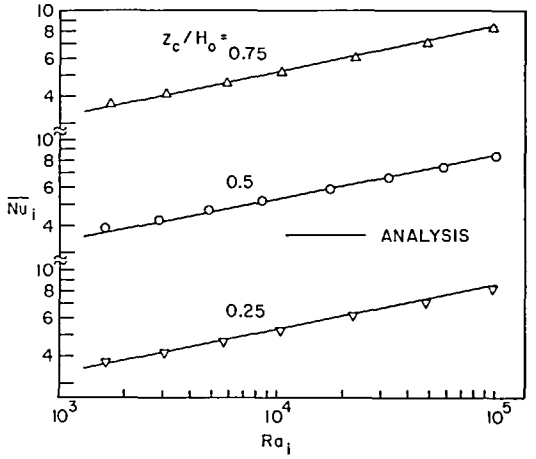

FIG. 3. Comparison of average inner-cylinder Nusselt numbers from experiment and analysis for the concentric case.

[1, 2]. In this regard, attention may be called to the algebraic correlations of the computed $\overline{Nu}_i$ that are presented in refs. [1, 2].

Very careful inspection of Fig. 3 suggests a possible slight difference in the slopes of the data and the prediction lines. This difference could be due to the limitation in the number of grid points available for the numerical solutions. Also, there may be a slight inaccuracy in the data at low Rayleigh numbers. For instance, at the lowest Rayleigh number, the temperature difference $T_i - T_o$ is equivalent to a thermocouple emf of 30 μV, and this difference was read with an instrument having a resolving capability of 1 μV.

The experimental results for an extended range of inner cylinder elevations for both concentric and eccentric positioning will now be examined. Figure 4 shows the results for concentric positioning and for seven different elevations between $z_c/H_o = 0.1375$ and 0.8625. The figure is subdivided into two graphs. The lower graph conveys results for the lower elevations $0.1375 \leqslant z_c/H_o \leqslant 0.5$, while the upper graph is for the higher elevations $0.5 \leqslant z_c/H_o \leqslant 0.8625$. The data for the mid-height position $z_c/H_o = 0.5$ are common to both graphs and are represented by blackened symbols for emphasis. These blackened symbols help to tie the two graphs together.

An overall inspection of Fig. 4 indicates that there is a very weak dependence of the Nusselt number on the elevation of the inner cylinder. Indeed, the Nusselt number is virtually independent of elevation for $Ra_i > 10^4$. The somewhat greater sensitivity to elevation that is in evidence for $Ra_i < 10^4$ may, in part, be due to data scatter caused by the 1 μV resolution of the thermocouple emf's. It may also be due to the increased role of direct heat conduction between the cylinders as natural convection wanes with decreasing Rayleigh number.

The aforementioned insensitivity is especially remarkable when note is taken of the close approach of the inner and outer cylinders when $z_c/H_o = 0.1375$ and 0.8625. For example, for $z_c/H_o = 0.1375$, the clearance gap between the lower face of the inner cylinder and the bottom of the outer cylinder is only 0.0375 H_o. A similar gap exists above the inner cylinder when $z_c/H_o = 0.8625$. Within such a narrow gap, it is expected that there would be direct heat conduction between the cylinders but very little natural convection. As the gap grows larger, the conduction will diminish and the natural convection will grow stronger. According to the Nusselt number results, it appears that the changes in these processes are in balance.

Results for eccentric positioning of the inner cylinder will now be presented. The eccentric positioning is illustrated in Fig. 1, where the radial stations r_{c2} and r_{c3} are respectively defined by $r_c/D_o = 0.25$ and 0.325. The closest radial approach of the two cylinders corresponding to the $r_c/D_o = 0.325$ case is just half the closest radial approach when $r_c/D_o = 0.25$.

The Nusselt number results for the eccentric mode are presented in Fig. 5, with those for $r_c/D_o = 0.25$ in the lower graph and those for $r_c/D_o = 0.325$ in the upper graph. For each case, data were collected for elevations $z_c/H_o = 0.1375$, 0.5, and 0.8625. For reference purposes, the mid-height data for the concentric mode are shown in both graphs as blackened circles.

From an examination of both graphs of Fig. 5 and

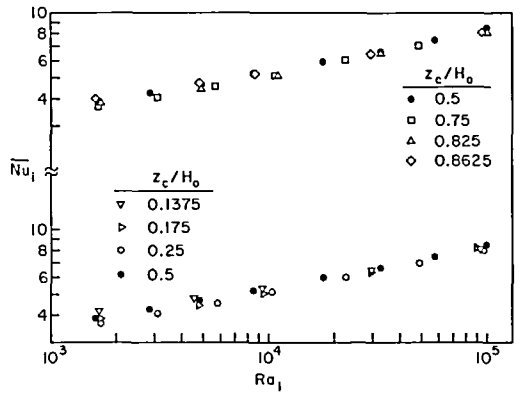

FIG. 4. Average inner-cylinder Nusselt numbers for various inner cylinder elevations, concentric case.

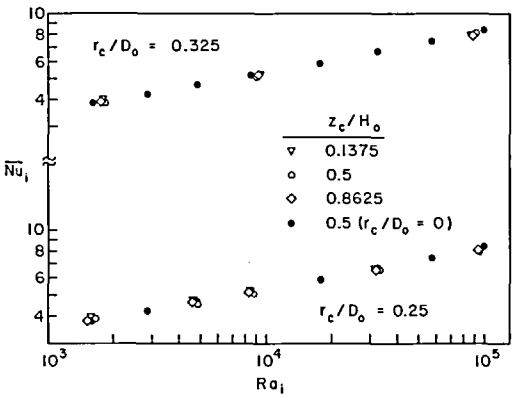

FIG. 5. Effect of eccentric positioning on the average inner-cylinder Nusselt number.

taking account of the blackened symbols, it appears that the Nusselt number is not affected by the eccentricity in the range investigated. Furthermore, the insensitivity of $\overline{Nu}_i$ to elevation, already noted in connection with Fig. 4, continues.

From the foregoing, it follows that in the investigated ranges of z_c/H_o and r_c/D_o, the average inner cylinder Nusselt number is independent of inner cylinder position. It should be emphasized that this finding pertains to the average heat transfer coefficient for the cylinder as a whole and is not applicable to the local coefficients.

By considering Figs. 4–6, it may also be concluded that all the data (for all investigated z_c/H_o and r_c/D_o values) are in very good agreement with the numerical predictions. Consequently, the algebraic correlation of the numerical results [1,2] can also be employed for the experimental results. This correlation is

$$\overline{Nu}_i = 0.820\, Ra_i^{0.204}, \quad Ra_i \geqslant 10^3. \tag{7}$$

It can also be argued that enclosure configurations characterized by D_i/D_o ratios smaller than the 0.2 value employed here should yield $\overline{Nu}_i$ that are also insensitive to inner cylinder position. Consequently, the correlated numerical results for $D_i/D_o < 0.2$ should have as broad a range of validity with regard to inner cylinder position as does equation (7). For $0.1 \leqslant D_i/D_o \leqslant 0.2$ and for $Ra_i \geqslant 10^3$, [1] gives

$$\overline{Nu}_i = 0.754(D_o/D_i)^{0.052} Ra_i^{0.204}. \tag{8}$$

Equation (8) is valid for all positions of the inner cylinder and is recommended for the aforementioned ranges of D_i/D_o and Ra_i.

ADDITIONAL ANALYTICAL RESULTS

Streamlines and isotherms

Insights into the fluid flow pattern and temperature distribution in the enclosure can be obtained by examination of streamline and isotherm maps. Representative streamline maps for $D_i/D_o = 0.2$ (the diameter ratio of the experiments) are presented in Figs. 6 and 7, while the corresponding temperature distributions are shown in Figs. 8 and 9. Figures 6 and 8 show results for the inner cylinder positioned at $z_c/H_o = 0.25$ (the lowest elevation at which numerical solutions were obtained), with left- and right-hand graphs which correspond respectively to $Ra_i = 10^3$ and 10^5. A similar presentation, but for $z_c/H_o = 0.75$ (the highest elevation investigated numerically), is made in Figs. 7 and 9. Streamlines and isotherms for the case of the inner cylinder at the mid-height position ($z_c/H_o = 0.5$) and for $D_i/D_o = 0.2$ are available [1].

Each graph is a side view of the enclosure and its bounding cylinders. Because of symmetry about the vertical axis, only the region between the axis and the wall of the outer cylinder need be shown. The right-hand boundary of each graph is the symmetry axis, while the left-hand boundary is the wall of the outer cylinder. In each graph, the inner cylinder appears as a rectangular region adjacent to the symmetry axis.

The numerical results presented in Figs. 6–9, as well as those of the subsequent figures, were purposely not included in the results of ref. [2] because they form a natural complement to the experimental results given in the present paper.

Inspection of the streamlines of Figs. 6 and 7 shows

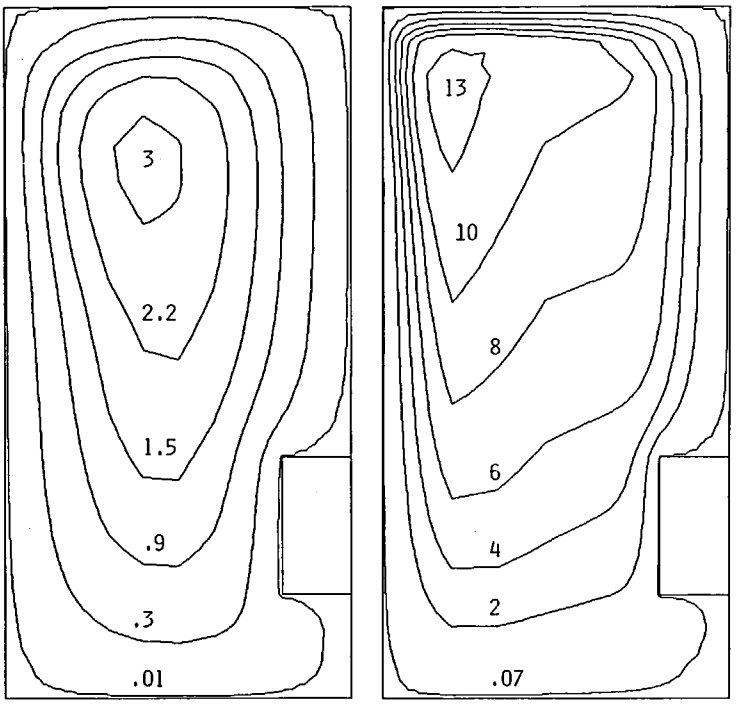

FIG. 6. Streamline maps corresponding to a concentric inner cylinder positioned at a low elevation ($z_c/H_o = 0.25$). Left-hand graph: $Ra_i = 10^3$; right-hand graph: $Ra_i = 10^5$.

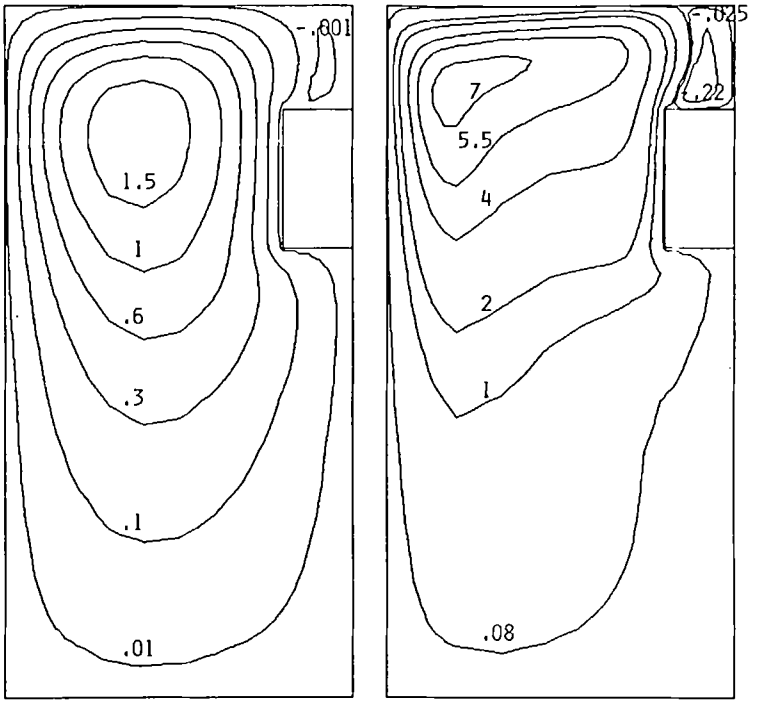

FIG. 7. Streamline maps corresponding to a concentric inner cylinder positioned at a high elevation ($z_c/H_o = 0.75$). Left-hand graph: $Ra_i = 10^3$; right-hand graph: $Ra_i = 10^5$.

that the dominant feature of the flow field is a general recirculation whereby the fluid moves upward adjacent to the inner cylinder and the symmetry axis and downward adjacent to the side wall of the outer cylinder. The eye of the recirculation is situated in the upper portion of the enclosure and, with increasing Rayleigh number, the eye moves outward toward the side wall of the outer cylinder.

An indication of the vigor of the recirculating flow can be obtained from the numerical values of the dimensionless stream function Ψ ($=\psi/\nu D_o$) that are used to label the respective streamlines. These

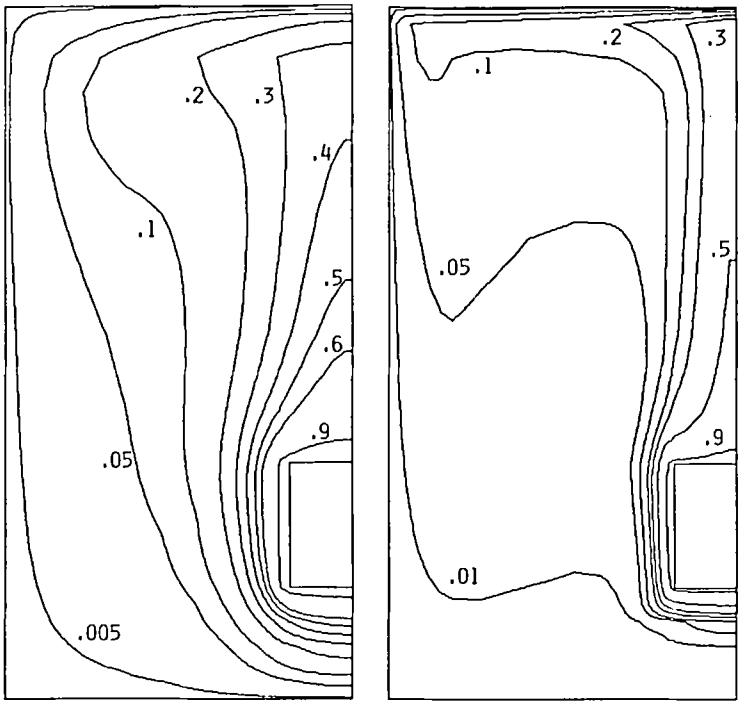

FIG. 8. Isotherm maps corresponding to a concentric inner cylinder positioned at a low elevation ($z_c/H_o = 0.25$). Left-hand graph: $Ra_i = 10^3$; right-hand graph: $Ra_i = 10^5$.

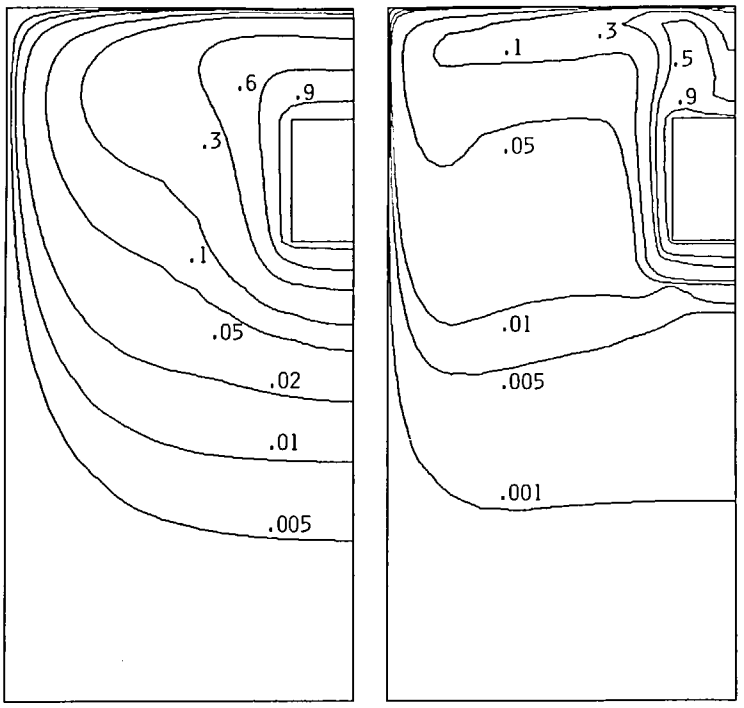

FIG. 9. Isotherm maps corresponding to a concentric inner cylinder positioned at a high elevation ($z_c/H_o = 0.75$). Left-hand graph: $Ra_i = 10^3$; right-hand graph: $Ra_i = 10^5$.

numerical values show that the velocities increase with increasing Rayleigh number, as is to be expected. Also, at higher Rayleigh numbers, there is a tendency for the streamlines to crowd together adjacent to certain of the surfaces of the enclosure, indicating the presence of a boundary layer type flow in those regions.

Of special interest with regard to the heat transfer results presented earlier in the paper are the changes in the pattern of the fluid flow which occur at a fixed Rayleigh number as the elevation of the inner cylinder is varied. It may be recalled that the average inner-cylinder heat transfer coefficient is quite insensitive to changes in inner cylinder elevation. On the other hand, an overview of Figs. 6–9 suggests that the fluid flow pattern is more sensitive to the elevation of the cylinder. When the cylinder is at a low elevation, it draws fluid downward to it, so that there is a vigorous flow in the lower portion of the enclosure. As a consequence, the vigor of the natural convection flow is more uniform throughout the enclosure at low inner cylinder elevations than at high inner cylinder elevations. In the latter case, the lower portion of the enclosure is occupied by a sluggish fluid flow.

An especially interesting flow pattern develops above the inner cylinder when it is situated at high elevations. For this positioning, the main recirculating flow is unable to penetrate the gap above the cylinder. Instead, the gap is filled with a local recirculation zone which has a downflow leg along the axis and an upflow leg adjacent to the main recirculation.

From the foregoing discussion, it is clear that there are certain large-scale differences between the flow fields for $z_c/H_o = 0.25$ and 0.75. However, very close inspection of the flow patterns immediately adjacent to the side and lower surfaces of the inner cylinder shows them to be relatively unaffected by the change in elevation, and this conclusion can be affirmed by study of the more detailed streamline maps presented in ref. [1]. If note is taken of the fact that most of the inner cylinder heat transfer takes place at the side and lower surfaces of the inner cylinder (Table 1 of ref. [2]), then the previously noted insensitivity of $\overline{Nu}_i$ to inner cylinder elevation can be rationalized.

In the isotherm maps of Figs. 8 and 9, the numerical values which label each of the contour lines in these figures correspond to the dimensionless temperature $(T-T_o)/(T_i-T_o) \equiv \theta$. The θ values at the inner and outer cylinders are, respectively, 1 and 0.

Inspection of Figs. 8 and 9 indicates that the temperature field in the enclosure is significantly affected by both the elevation of the inner cylinder and the Rayleigh number. With the inner cylinder at a low elevation and at $Ra_i = 10^3$ (left-hand graph of Fig. 8), there is little stratification in evidence, and the boundary layer adjacent to the inner-cylinder side wall is rather thick. For this same inner cylinder elevation and at $Ra_i = 10^5$, stratification has set in, as evidenced by the horizontal isotherms, and the boundary layer has become thinner. Furthermore, aside from the neighborhood of the inner cylinder and the corridor which extends upward from it, most of the enclosure is filled with fluid whose temperature is very near the temperature T_o of the outer cylinder.

When the inner cylinder is positioned at a high

elevation (Fig. 9), the lower portion of the enclosure contains fluid whose temperature is not very different from T_o, and there is increasing stratification at higher Rayleigh numbers. An increase in Rayleigh number also leads to a thinning of the thermal boundary layer below and at the side of the inner cylinder, while the isotherm pattern above the cylinder reflects the local recirculation zone identified in Fig. 7.

Despite the large-scale differences in the temperature field which accompany a change in the inner cylinder elevation at a fixed Rayleigh number, the isotherm pattern immediately adjacent to the inner cylinder is hardly changed. This behavior is consistent with the insensitivity of the measured average heat transfer coefficients to changes in elevation.

Heat transfer results

As noted earlier, a listing of the numerically predicted average Nusselt numbers $\overline{Nu}_i$ for the inner cylinder is available in Table 2 of ref. [2] [note that $\overline{Nu}_o$ can be obtained from $\overline{Nu}_i$ by means of equation (3)]. In addition, the average coefficients for the individual surfaces (bottom, side, and top) of both the inner and outer cylinders are given in Table 1 of the same reference. Here, representative results will be presented for the distributions of the *local* heat transfer coefficients on the bottom, side, and top surfaces of the inner cylinder. These results pertain to the diameter ratio $D_i/D_o = 0.2$ of the experiments. A more complete presentation of local coefficient distributions can be found in ref. [1].

The distributions of the local Nusselt number Nu_i are plotted in Figs. 10 and 11. The first of these figures displays the effect of Rayleigh number at a fixed inner cylinder elevation, while the second shows the effect of elevation variations at a fixed Rayleigh number. Figure 10 corresponds to an inner cylinder elevation $z_c/H_o = 0.5$ (mid-height). The two lower graphs convey results for $Ra_i = 10^3$, while the two upper graphs are for $Ra_i = 10^5$. The lines labeled b, s, and t correspond to the bottom, side, and top surfaces of the inner cylinder. Also

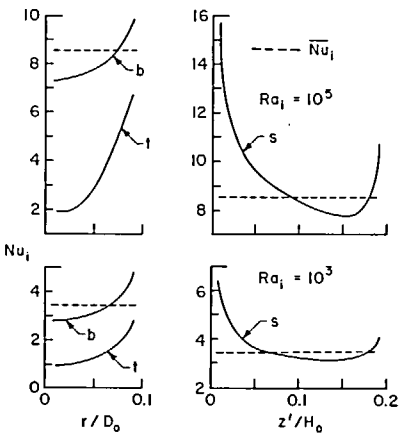

FIG. 10. Effect of Rayleigh number on the local Nusselt number distributions on a concentric inner cylinder positioned at mid-height.

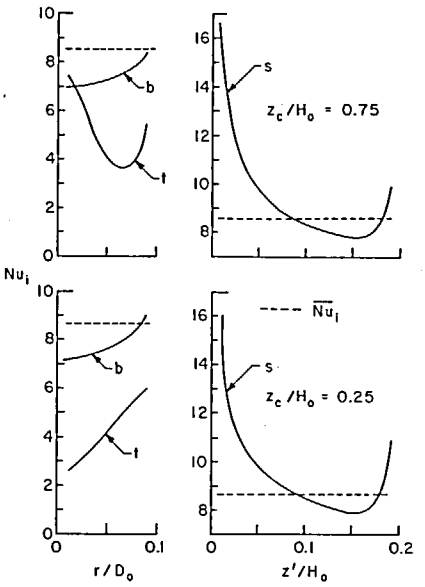

FIG. 11. Effect of elevation on the local Nusselt number distributions on a concentrically positioned inner cylinder, $Ra_i = 10^5$.

appearing in each of the graphs is a reference line (dashed) which represents the average Nusselt number $\overline{Nu}_i$ for the inner cylinder as a whole. The r coordinate of the left-hand graphs measures radial distances from the axis; in the right-hand graphs, z' measures distances upward from the lower edge of the inner cylinder.

From Fig. 10, it is seen that the heat transfer coefficients at both the top and bottom surfaces increase in the radial outward direction, with those on the bottom surface being larger in magnitude. Along the side of the cylinder, the coefficient takes on a maximum at the leading edge and decreases in the upward direction (i.e. in the flow direction), as is appropriate for a boundary layer flow. Near the upper end of the cylinder, the downward trend of Nu_i is reversed as the flow moves radially inward and tries to penetrate the space above the cylinder.

With regard to the Rayleigh number, a primary effect is to increase the magnitudes of the local coefficients. In addition, the sharpness of the dropoff of the coefficient along the side surface is accentuated, as is the rise which occurs adjacent to the upper end of the side. The extent of the variation of Nu_i along the top surface is also accentuated at higher Ra_i.

Figure 11 pertains to $Ra_i = 10^5$, with lower graphs which correspond to $z_c/H_o = 0.25$ and upper graphs which correspond to $z_c/H_o = 0.75$. The figure shows that the Nu_i distributions along the bottom and side surfaces are very little affected by the change of elevation of the inner cylinder. However, there is a marked difference in the Nu_i distribution at the top surface due to the elevation-related change in the fluid flow pattern. Since the heat transfer rates at the side and bottom surfaces substantially exceed that at the top surface, the average Nusselt number $\overline{Nu}_i$ is nearly immune to the change in the top-surface local Nusselt number distribution.

CONCLUSIONS

This paper has reported results for natural convection heat transfer in the enclosed space between two vertical cylinders of different height and diameter. The experimental portion of the work was performed for both concentric and eccentric positioning of the inner cylinder, while the numerical work was limited to the concentric case. The experiments constitute the main focus of the paper, but numerically predicted results are also presented to complement the experimental results.

During the course of the experiments, the vertical position of the inner cylinder was varied systematically from a low elevation in the enclosure to a high elevation in the enclosure. In addition to the concentric positioning of the inner cylinder, two eccentric positions were employed. For each geometrical configuration, the inner cylinder Rayleigh number was varied over the range from 1.5×10^3 to 10^5. All the experiments were performed for an inner cylinder to outer cylinder diameter ratio D_i/D_o of 0.2. The heights of the cylinders were equal to their respective diameters.

The measurements yielded the average Nusselt number $\overline{Nu}_i$ for the inner cylinder [equation (3) relates the outer cylinder Nusselt number to $\overline{Nu}_i$]. A comparison of the experimentally determined concentric-mode $\overline{Nu}_i$ values with the numerical predictions yielded excellent agreement between the two sets of results, with most of the data falling within 1% of the prediction lines. This level of agreement lends support both to the experimental technique and to the numerical methodology. In particular, the validity of the numerical results for diameter ratios other than $D_i/D_o = 0.2$ is established by inference.

When all of the experimental results are considered, it may be concluded that the average Nusselt number is quite insensitive to the geometrical parameters of the enclosure (i.e. the inner cylinder elevation and eccentricity). Therefore, a Nusselt–Rayleigh correlation can be obtained which is free of the aforementioned geometrical parameters. Such a correlation is conveyed by equation (7) for $D_i/D_o = 0.2$. The insensitivity of $\overline{Nu}_i$ to elevation and eccentricity should continue to prevail for $D_i/D_o < 0.2$, and a $\overline{Nu}_i$–Ra_i correlation for the range $0.1 \leqslant D_iD_o \leqslant 0.2$ is given by equation (8).

Additional complementary numerical results presented in the paper include streamline and isotherm maps and local heat transfer coefficients, all for $D_i/D_o = 0.2$. The streamline and isotherms show that whereas there are elevation-related changes in the flow and temperature fields, there is little effect adjacent to the side and bottom surfaces of the inner cylinder. Similarly, the distributions of the local Nusselt numbers along these surfaces are little influenced by the changes in elevation. The upper surface is more affected, but it contributes relatively little to the overall heat transfer from the inner cylinder as a whole.

REFERENCES

1. M. Charmchi, Experimental and analytical study of natural convection in the enclosed space between finite length cylinders, Ph.D. Thesis, Department of Mechanical Engineering, University of Minnesota, Minneapolis, Minnesota (1981).
2. M. Charmchi and E. M. Sparrow, Analysis of natural convection in the space between concentric vertical cylinders of different height and diameter, *Numer. Heat Transfer* 5, 119–144 (1982).
3. E. M. Sparrow and R. D. Cess, *Radiation Heat Transfer*, p. 80. Hemisphere, Washington, D.C. (1978).

EXPERIENCES DE CONVECTION NATURELLE DANS UNE ENCEINTE ENTRE DES CYLINDRES VERTICAUX CONCENTRIQUES OU NON, DE DIAMETRES ET DE HAUTEURS VARIES

Résumé—On détermine expérimentalement les coefficients de transfert thermique pour la convection naturelle dans l'espace fermé entre deux cylindres verticaux, maintenus à des températures différentes et uniformes. Les cylindres ont différentes hauteurs et diamètres. Au cours des expériences, le positionnement vertical (l'élévation) du cylindre intérieur et son excentricité sont rendus variables. Pour chaque configuration le nombre de Rayleigh de cylindre intérieur varie entre $1{,}5 \times 10^3$ et 10^5. Le fluide de transfert est l'air. Pour compléter l'étude expérimentale, des résultats numériques obtenus pour différentes solutions sont présentés dans le cas concentrique. Des comparaisons entre expérience et théorie montrent un accord qui, pour la plupart, est inférieur à un pour cent. En général, le nombre de Nusselt moyen est presque indépendant à la fois de l'élévation et de l'excentricité du cylindre intérieur. Ceci permet de relier le nombre de Nusselt au nombre de Rayleigh et au rapport des diamètres des cylindres, sans tenir compte de l'élévation et de l'excentricité.

UNTERSUCHUNG DER NATÜRLICHEN KONVEKTION IM HOHLRAUM ZWISCHEN EXZENTRISCHEN ODER KONZENTRISCHEN SENKRECHTEN ZYLINDERN VON VERSCHIEDENER HÖHE UND DURCHMESSER

Zusammenfassung—Es wurden die Wärmeübergangskoeffizienten bei der natürlichen Konvektion im Hohlraum zwischen zwei senkrechten Zylindern, die auf unterschiedlicher aber einheitlicher Temperatur gehalten werden, experimentell bestimmt. Die Zylinder waren sowohl von unterschiedlicher Höhe als auch von unterschiedlichem Durchmesser. Im Verlauf der Experimente wurde die senkrechte Positionierung (d.h. die Erhöhung) des inneren Zylinders und seine Exzentrizität als Parameter variiert. Für jede Hohlraumkonfiguration bewegte sich die Rayleighzahl im Innenzylinder im Bereich von $1{,}5 \times 10^3$ bis 10^5 Das wärmeübertragende Medium war Luft. Zur Ergänzung der experimentellen Arbeiten werden für den konzentrischen Fall numerische Ergebnisse dargestellt, die mittels finiter Differenzen erhalten worden sind. Vergleiche zwischen den experimentellen und numerischen Ergebnissen ergaben eine Übereinstimmung, die meistens innerhalb eines Prozentes lag. Im allgemeinen war die mittlere Nusseltzahl nahezu unabhängig von der Erhöhung und der Exzentrizität des inneren Zylinders. Diese Erkenntnis ermöglichte eine Korrelation der Nusseltzahl als Funktion der Rayleighzahl und dem Durchmesserverhältnis der Zylinder ohne Berücksichtigung der Erhöhung und der Exzentrizität.

ЭКСПЕРИМЕНТАЛЬНОЕ ИССЛЕДОВАНИЕ ЕСТЕСТВЕННОЙ КОНВЕКЦИИ В ЗАМКНУТОМ ОБЪЕМЕ МЕЖДУ ЭКСЦЕНТРИЧЕСКИМИ ИЛИ КОНЦЕНТРИЧЕСКИМИ ВЕРТИКАЛЬНЫМИ ЦИЛИНДРАМИ РАЗЛИЧНОЙ ВЫСОТЫ И ДИАМЕТРА

Аннотация—Экспериментально определены коэффициенты теплопереноса при естественной конвекции в замкнутом объеме между двумя вертикальными цилиндрами с различной, но постоянной температурой. Цилиндры имели разную высоту и диаметр. Во время экспериментов вертикальное положение (подъем) внутреннего цилиндра и его эксцентриситет изменялись параметрически. Для каждой конфигурации полости число Рэлея для внутреннего цилиндра изменялось в диапазоне от $1{,}5 \times 10^3$ до 10^5. Рабочей средой служил воздух. Помимо экспериментальных данных для концентрического случая представлены численные результаты, полученные методом конечных разностей. В большинстве случаев экспериментальные данные совпадают с численными в пределах 1%. Оказалось, что среднее число Нуссельта слабо зависит как от подъема, так и несоосности цилиндров. Это позволило построить зависимость числа Нуссельта только от числа Рэлея и отношения диаметров цилиндров без учета подъема и эксцентриситета.